AIP | APL Materials

Large acoustic thermal hysteresis in relaxor ferroelectric Pb(Zn1/3Nb2/3)O3-PbTiO3

Shinya Tsukada, Tae Hyun Kim, and Seiji Kojima

Citation: APL Materials **1**, 032114 (2013); doi: 10.1063/1.4821624
View online: http://dx.doi.org/10.1063/1.4821624
View Table of Contents: http://scitation.aip.org/content/aip/journal/aplmater/1/3?ver=pdfcov
Published by the AIP Publishing

APL MATERIALS **1**, 032114 (2013)

Large acoustic thermal hysteresis in relaxor ferroelectric $Pb(Zn_{1/3}Nb_{2/3})O_3$-$PbTiO_3$

Shinya Tsukada,[1,a] Tae Hyun Kim,[2] and Seiji Kojima[2,a]
[1]*Faculty of Education, Shimane University, Matsue city, Shimane 690-8504, Japan*
[2]*Pure and Applied Sciences, University of Tsukuba, Tsukuba city, Ibaraki 305-8573, Japan*

(Received 9 April 2013; accepted 2 July 2013; published online 19 September 2013)

The diffuse phase transition in relaxor-based $0.93Pb(Zn_{1/3}Nb_{2/3})O_3$–$0.07PbTiO_3$ ferroelectric single crystals is studied by observing the large thermal hysteresis over 100 K of the longitudinal acoustic (LA) phonon. By observing this hysteresis in the LA phonon frequency with different temperature-cycles, it is concluded that nonequilibrium states are induced by supercooling. Relaxor ferroelectrics easily go supercooling, because they demonstrate structural hierarchy like glass-forming materials. The inhomogeneous structure disrupts sharp phase transitions, revealing diffuse phase transition on cooling. However, annealing at low temperatures reduces the inhomogeneity markedly. These interpretations are consistent with LA phonon behavior under electric fields, which reduce the inhomogeneity. [http://dx.doi.org/10.1063/1.4821624]

Inhomogeneous systems attract a great deal of research in the field of condensed matter physics, as intrinsic inhomogeneities in complex oxides often induce substantial effects, such as giant dielectric and electromechanical responses in relaxor ferroelectrics.[1]

Relaxor ferroelectrics are a special class of ferroelectrics whose dielectric responses demonstrate broad maxima with variations in temperature and frequency. A unique property of these materials is the appearance of local and randomly oriented ferroelectric regions several nanometers wide; these regions are termed polar nanoregions (PNR).[1,2] In addition, static nanodomain and microdomain structures are observed;[3–5] that is, relaxor ferroelectrics demonstrate structural hierarchy. Although the response of homogeneous dielectric materials to an external electric field is usually related to ionic displacements, relaxor ferroelectrics show high-order structure at a mesoscopic scale—such as PNRs, nanodomains, and microdomains—such that their responses are enhanced by their fluctuations, leading to very large piezoelectric and dielectric constants. Thus, relaxor ferroelectrics are an intriguing system in which intrinsic inhomogeneity can lead to a large-magnitude response to an external electric field.

Typical relaxor ferroelectrics are $Pb(B'B'')O_3$–$PbTiO_3$, $(Sr_{1-x}Ba_x)Nb_2O_6$, and $(K_3Li_{2-x})Nb_{5+x}O_{15+2x}$, where the common features of their chemical formulae are random arrangements of different ions on crystallographically equivalent sites. It is known that frustration between the electrical instability and the spatial instability is the cause of the relaxor phenomena. A simple consideration of $Pb(B'B'')O_3$–$PbTiO_3$ shows that a 1:1 order in the B-sites of the perovskite structure reduces strain, while a 1:2 order is required for charge neutrality. As a result, the B-site inevitably becomes random. The randomly oriented local electric and elastic fields generate the PNRs as the precursor clusters of a ferroelectric phase transition. The PNRs are understood in connection with phase transitions using four temperatures, from the highest to the lowest: (i) the Burns temperature, T_B, at which dynamic PNRs appear; (ii) the intermediate temperature, T^*, below which static PNRs begin to appear; (iii) the frequency-dependent temperature at the dielectric peak,

[a]Authors to whom correspondence should be addressed. Electronic addresses: tsukada@edu.shimane-u.ac.jp and kojima@ims.tsukuba.ac.jp

T_m; and (iv) the ferroelectric phase-transition temperature, T_C [or the freezing temperature T_f in the case when this transition is absent, as in $Pb(Mg_{1/3}Nb_{2/3})O_3$ (PMN)].

Various investigations of relaxor ferroelectrics have been undertaken to understand the curious phenomena described above. The characteristic properties of these materials have been attributed to several causes, depending on the length scale. For example, local ionic displacements at the cores of PNRs were confirmed by diffraction measurements.[6] The appearance of dynamic PNRs deviates from the usual linear temperature dependence of the refractive index and sound velocity.[2,7,8] When dynamic PNRs freeze into static ones, an acoustic emission burst is observed.[9,10] Static PNRs change the thermal expansion behavior.[3,11] The alignment of the static PNRs determines the macroscopic ferroelectricity,[12] and ferroelectric domain arrangement induces the observed colossal piezoelectricity.[13] Thus, at the present stage of research, it is important to connect each phenomenon with structural morphology.

In the present study, inelastic light scattering from a longitudinal acoustic (LA) phonon in $(1-x)Pb(Zn_{1/3}Nb_{2/3})O_3$–$xPbTiO_3$ single crystals (PZN–xPT) was measured: we found marked thermal hysteresis in the LA phonon frequency over 100 K in PZN–0.07PT. To illustrate the behavior of the hysteresis, which is much larger than noted in previous works,[8,14,15] we measured it over different temperature cycles and connected this phenomenon with the structural morphology and phase stability. To support our mesoscopic picture and explain the hysteresis, measurements of the LA phonon of PZN–0.045PT under an electric field were performed.

Single crystals of PZN–0.045PT and PZN–0.07PT were grown using the high-temperature flux technique with PbO-based fluxes (Microfine Materials Technologies). Each surface of the crystals was a (100) plane of pseudo-cubic orientation. The LA phonon close to the Γ point of reciprocal space was observed through inelastic light scattering. The light scattering was measured with a high-contrast 3 + 3-pass tandem Fabry–Pérot interferometer (JRS Scientific Instruments) combined with an optical microscope (Olympus). A diode-pumped solid-state laser (Coherent Inc.) with single-frequency operation at 532 nm and an output power of 100 mW was used. A 180° scattering geometry without a polarizer was adopted for observing the LA phonon.

The sample was placed inside a cryostat cell (Linkam Scientific Instruments) to allow the sample temperature to be adjusted between 80 K and 873 K; measurements were performed with various thermal cycles. The complex dielectric constant ($\varepsilon^* = \varepsilon' - j\varepsilon''$) of a PZN–0.07PT single crystal was measured using an impedance/gain-phase analyzer (Solartron) in the $[100]_C$ direction. The measurements were performed while cooling and heating at a rate of 1 K min^{-1} in a homemade furnace.

Figure 1 shows the contour map of light scattering spectra of PZN–0.07PT as functions of the frequency shift and temperature. The scattering was measured upon cooling, then measured on heating. The data on cooling were reported in our previous paper.[16] The spectrum consists of an LA phonon at ±42 GHz, which is related to the complex elastic stiffness constant $c_{11}{}^* = c_{11}{}' - jc_{11}{}''$, and a central peak at 0 GHz, which is related to relaxation in the GHz range. Transverse acoustic phonons do not appear due to the symmetry restriction of the cubic photoelastic tensor. Temperature-dependent inelastic scattering from the LA phonon is clearly observed at all temperatures in Fig. 1. The dark portions at 0 GHz denote elastic scattering.

The figure shows a clear anomaly in the LA phonon around 400 K: the LA phonon softens toward T_C on both cooling and heating runs. At the same time, the peak broadens towards T_C. The anomalous behavior is typical of ferroelectric phase transitions in perovskite ferroelectrics through strain–polarization coupling of free energy. However, the temperature range over which the phonon anomaly is observed in Fig. 1 is especially large for the cubic perovskite structure, reflecting the characteristics of relaxor ferroelectrics.

The analyzed results of the spectra in Fig. 1 are shown in Fig. 2(a); the fitting procedure has been described in our previous works.[7,8,16] The calculated parameters of the LA phonons—including the Brillouin shift (ν_B) and the full-width at half-maximum (FWHM, abbreviated as Γ)—represent the characteristic tendencies of the LA phonon (i.e., softening over a wide temperature range and thermal hysteresis) more clearly than Fig. 1. Above T_C, typical perovskite ferroelectrics do not show an anomaly in the LA phonon, or only show anomalies in a narrow temperature range less than 10 K wide, because the piezoelectric coupling is prohibited in their paraelectric phases due to the

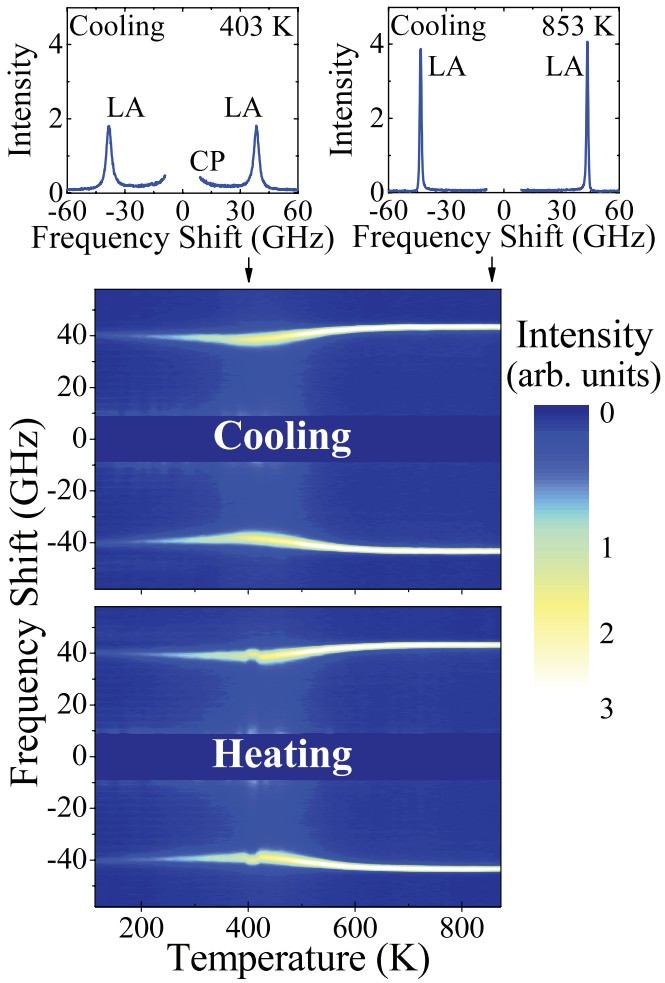

FIG. 1. Contour map of inelastic light scattering intensity from PZN–0.07PT versus temperature and frequency shift in $x(z\ y+z)\bar{x}$ scattering geometry (free spectral range = 75 GHz, scan range = 70.5 GHz).

symmetry restriction. Consequently, the LA phonon anomaly in the relaxor ferroelectrics indicates that strong coupling between strain fluctuation and polarization fluctuation exists in the relaxor ferroelectrics.[17,18] Taking the local structure of the PNR into account, we attribute this anomaly in a broad temperature range to the piezoelectric coupling inside the PNRs. Because the local structure inside the PNRs is noncentrosymmetric,[19,20] even though the matrix around the disorder is centrosymmetric, the polarization fluctuation can couple linearly with the strain fluctuation.[16,21] Although the PNRs are smaller than the wavelength of light, the macroscopic properties of the material can be influenced by local structure through coupling.

Figure 2(a) also shows an apparent thermal hysteresis around 400 K in the LA phonon; that is, the ν_B on heating shows two discontinuous points at 398 K and 420 K, while only one minimum at 390 K is shown in the data on cooling. These temperatures correspond to the structural phase transition temperatures, $T_{T-R} \approx 400$ K and $T_{C-T} \approx 420$ K ($=T_C$), which were determined by measuring ε^* upon heating after poling.[22] Therefore, the discontinuities in ν_B upon heating are caused by macroscopic changes in the structure.

Thermal hysteresis is also shown in the dielectric constant, $\varepsilon^* = \varepsilon' - j\varepsilon''$. Figure 2(b) represents jumps in the ε' and ε'' at 388 K on a cooling run (T_C^{Cool}) and at 419 K on a heating run (T_C^{Heat}), where jumps in the ε' and ε'' are regarded as occurring at values of T_C.[23,24] The temperature T_C^{Cool} is in good agreement with the minimum temperature of ν_B measured on cooling, while T_C^{Heat} is in good agreement with the minimum temperature of ν_B measured on heating ($=T_{C-T}$). Thus, the dielectric

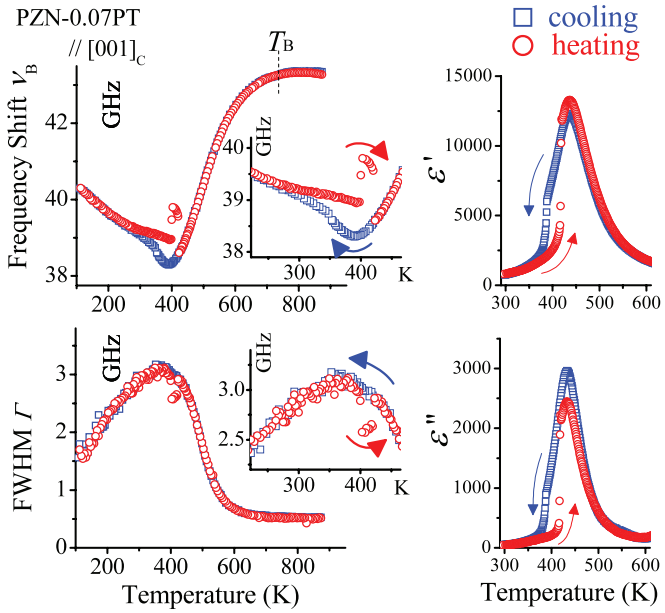

FIG. 2. (a) Frequency shift, ν_B, and FWHM, Γ, of the Brillouin scattering, which are determined by fitting the spectra in Fig. 1. The thermal hysteresis observed around 400 K is enlarged in the insets. (b) Real and imaginary parts of the complex dielectric constants ε' and ε''.

measurement proves that the minimum temperature in ν_B (Fig. 2(b)) is the Curie temperature where the ferroelectric phase transition occurs. Note that Brillouin scattering measurement probes an acoustic wave at GHz range. Because domain and domain boundary fluctuations appear up to MHz range in the ferroelectric phase, the change at the ferroelectric to ferroelectric phase transition is smeared in the dielectric measurement.

The temperature dependence of ν_B and Γ is reproducible on thermal cycles. Figure 3 shows ν_B during different thermal cycles. Once the sample is heated above T_C^{Heat}, the memory of the previous treatment disappears, as shown in Fig. 3(a). Figure 3(b) demonstrates the dependence of the lower temperature limit of the cycle on the hysteresis. When the lower temperature limit is low enough, the hysteresis loop clearly appears. On the other hand, when the lower temperature limit is not low enough, the hysteresis loop behaves differently from the larger loop. The thermal hysteresis in ν_B observed in the 5th and 6th runs in Fig. 3(b) is quite similar to that observed in previous works on relaxor ferroelectrics with cubic–rhombohedral phase transitions.[8,14,15] This indicates that a cubic phase transforms into a rhombohedral state under nonequilibrium condition at 388 K on cooling for the 5th run, then the rhombohedral state into a cubic phase for the 6th run.

Xu *et al.* measured the neutron diffuse scattering from PZN–0.08PT upon cooling under the applied electric field, then the sample was heated without applying the electric field.[25] They investigated the temperature at which the effect of the applied electric field disappears. Their result indicated that the memory effect disappears around 510 K ($>T^*$) on heating, not the $T_C \approx 450$ K of PZN–0.08PT, which is different from our present result in which the memory effect disappears at T_C^{Heat}. Their interpretation was that atomic motions associated with the PNRs can remember the previous treatment even above T_C. Their diffuse scattering was probed at a length scale of an ionic displacement. However, the LA phonon measurement in this study probes at a length scale of the wavelength of light (∼100 nm). Therefore, the local memory inside the PNRs does not have an impact on the LA phonon thermal hysteresis.

Thermal hysteresis is normally considered to be one of the basic characteristics of a first-order phase transition. In this work, in PZN–0.07PT, a large thermal hysteresis is observed because two first-order phase transitions occur in a narrow temperature range. In general, more than one minimum in the free energy is thought to explain a first-order phase transition, but in the present case, at least three phases—cubic, tetragonal, and rhombohedral—should be taken into account. These phases

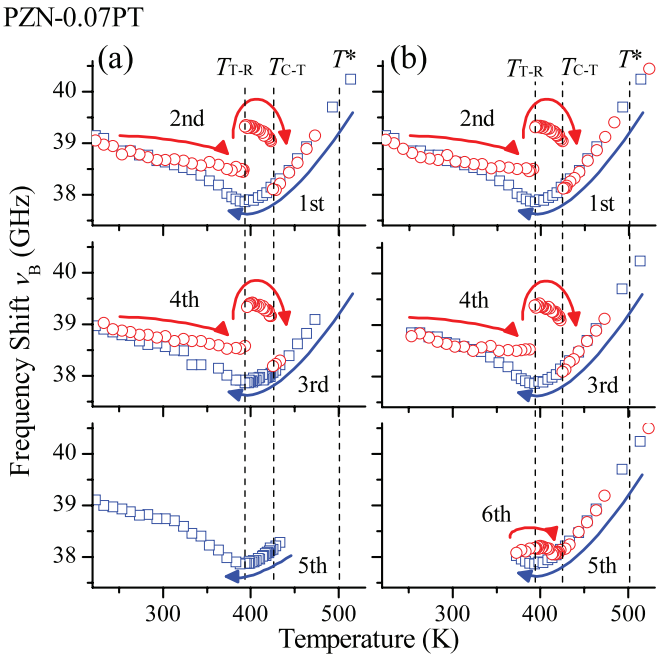

FIG. 3. Temperature dependences of ν_B with different thermal cycles. (a) The dependence of the higher temperature limit of the cycle on the hysteresis is shown. The upper figure shows the cycle from 823 K to 113 K (1st run), then to 473 K (2nd run). The middle figure shows the cycle from 473 K to 113 K (3rd run), then to 433 K (4th run). The bottom figure demonstrates the cycle from 433 K to 113 K (5th run). Here, T_{C-T} and T_{T-R} denote the structural phase transition temperatures on the heating run. (b) The dependence of the lower temperature limit of the cycle on the hysteresis is shown. The upper figure shows the cycle from 823 K to 113 K (1st run), then to 823 K (2nd run). The middle figure shows the cycle from 823 K to 253 K (3rd run), then to 823 K (4th run). The bottom figure demonstrates the cycle from 823 K to 373 K (5th run), then to 523 K (6th run). The data for the 3rd and 5th cooling runs were copied from the 1st run.

adopt similar free energies around the phase transitions; as a result, nonequilibrium states can be easily achieved through supercooling, leading to the appearance of the large thermal hysteresis. To illustrate the hysteresis in Fig. 4, free energies are assumed for each phase. When the sample is cooled from the high temperature (A), the cubic phase changes to a rhombohedral state at $T_C^{Cool} = 388$ K (B) under the nonequilibrium condition, and then the supercooled rhombohedral state becomes stable below 260 K (C). After keeping it at a low temperature (D), the sample is heated to a high temperature again. The rhombohedral phase remains stable below 400 K, above which the rhombohedral phase changes to the stable tetragonal phase (E). Finally, the tetragonal phase transforms into a stable cubic phase at $T_C^{Heat} = 420$ K (F). To confirm the stability of the supercooled state around 400 K on cooling (~B), the Brillouin scattering was measured before and after annealing for 10 h at 400 K. However, no change was found, indicating that nonequilibrium polymorphic states generated in the system have long lifetimes.

From a mesoscopic point of view, the inhomogeneous structure from the static PNRs, nanodomains, and microdomains can be attributed to phase transition diffuseness.[26] When the relaxor ferroelectrics are cooled across T_C from the highest temperature, the size of the inhomogeneity just below T_C must be distributed, which smears the phase transition, making it appear broad. Once the sample is cooled to much lower than T_C, the static PNRs, nanodomains, and microdomains unite with others, and thus the ferroelectric domains grow in size and in polarization. As a result, when the temperature is raised from a low temperature, the complex inhomogeneous structure is eliminated, making the phase transitions sharp. The effect of inhomogeneity on phase transition behavior is not so large in normal ferroelectrics. However, in the case of PZN–0.07PT, the cubic, tetragonal, and rhombohedral phases are in such competition around 400 K, in addition to the inhomogeneous structure, that the inhomogeneity can have a greater influence on the phases.

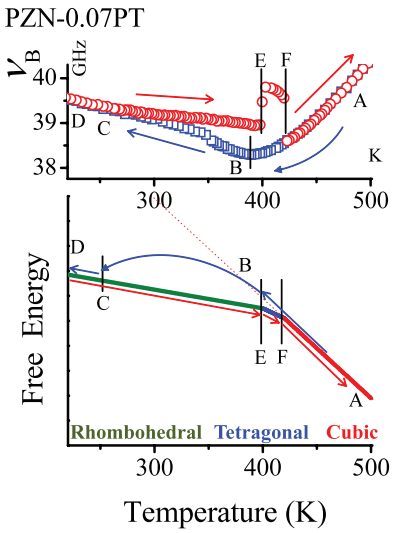

FIG. 4. (a) Thermal hysteresis in ν_B and (b) schematic of free energies predicted for PZN–0.07PT around the phase transition temperatures to explain the observed thermal hysteresis. The energies of the three phases are so close that supercooling can easily occur.

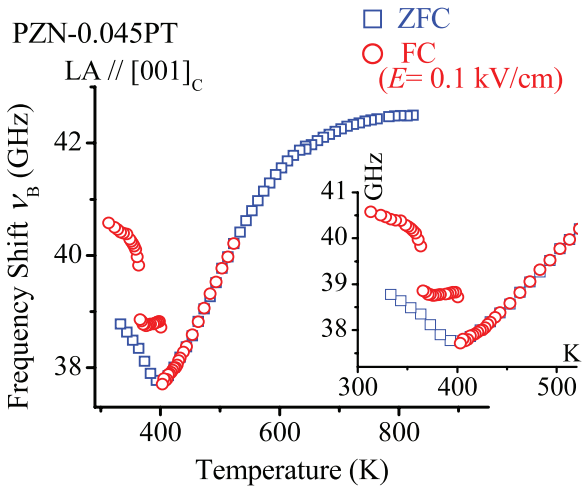

FIG. 5. Temperature dependence of ν_B of PZN–0.045PT upon zero-field cooling (ZFC) and field cooling (FC) with $E = 0.1$ kV/cm. The difference between ZFC and FC in ν_B is enlarged in the inset.

The above discussion on the relationship between phase transitions and inhomogeneous structure can also be understood in terms of the LA phonon measurement under an external electric field, because the electric field causes the static PNRs, nanodomains, and microdomains to grow into larger ferroelectric domains. Figure 5 shows the temperature dependence of ν_B of PZN–0.045PT with and without the electric field applied along the $[100]_C$ direction. The ν_B on field cooling shows similar sharp phase transitions to that on zero-field heating in PZN–0.07PT, while ν_B on zero-field cooling resembles that on zero-field cooling in PZN–0.07PT. This result indicates that the inhomogeneity is reduced by the electric field. From a thermodynamic point of view, the electric field enhances the relaxation from the nonequilibrium polymorphic states to the equilibrium homogeneous state.

We would like to thank Y. Akishige, K. Ohwada, M. Iwata, and J.-H. Ko for stimulating discussions. Financial support from the Electric Technology Research Foundation of Chugoku and the Grant-in-Aid for Young Scientists (B) program from MEXT, Japan is also gratefully acknowledged.

[1] A. A. Bokov and Z.-G. Ye, J. Mater. Sci. **41**, 31 (2006).
[2] G. Burns and B. A. Scott, Solid State Commun. **13**, 423 (1973).
[3] V. V. Shvartsman and A. L. Kholkin, Phys. Rev. B **69**, 014102 (2004).
[4] Z.-G. Ye, Curr. Opin. Solid State Mater. Sci. **6**, 35 (2002).
[5] M. Iwata, K. Katsuraya, I. Suzuki, M. Maeda, N. Yasuda, and Y. Ishibashi, Jpn. J. Appl. Phys. **42**, 6201 (2003).
[6] G. Xu, Z. Zhong, H. Hiraka, and G. Shirane, Phys. Rev. B **70**, 174109 (2004).
[7] S. Tsukada and S. Kojima, Phys. Rev. B **78**, 144106 (2008).
[8] S. Tsukada, Y. Ike, J. Kano, T. Sekiya, Y. Shimojo, R. Wang, and S. Kojima, J. Phys. Soc. Jpn. **77**, 033707 (2008).
[9] E. Dul'kin, M. Roth, P. E. Janolin, and B. Dkhil, Phys. Rev. B **73**, 012102 (2006).
[10] M. Roth, E. Mojaev, E. Dul'kin, P. Gemeiner, and B. Dkhil, Phys. Rev. Lett. **98**, 265701 (2007).
[11] B. Dkhil, P. Gemeiner, A. Al-Barakaty, L. Bellaiche, E. Dul'kin, E. Mojaev, and M. Roth, Phys. Rev. B **80**, 064103 (2009).
[12] I.-K. Jeong, J. K. Lee, and R. H. Heffner, Appl. Phys. Lett. **92**, 172911 (2008).
[13] T. Liu and C. Lynch, Continuum Mech. Thermodyn. **18**, 119 (2006).
[14] J.-H. Ko, D. H. Kim, S. Kojima, W. Z. Chen, and Z.-G. Ye, J. Appl. Phys. **100**, 066106 (2006).
[15] M. H. Kuok, S. C. Ng, H. J. Fan, M. Iwata, and Y. Ishibashi, Appl. Phys. Lett. **78**, 1727 (2001).
[16] S. Tsukada, Y. Hidaka, S. Kojima, A. A. Bokov, and Z.-G. Ye, Phys. Rev. B **87**, 014101 (2013).
[17] W. Rehwald, Adv. Phys. **22**, 721 (1973).
[18] S. Wakimoto, C. Stock, Z. G. Ye, W. Chen, P. M. Gehring, and G. Shirane, Phys. Rev. B **66**, 224102 (2002).
[19] N. W. Thomas, S. A. Ivanov, S. Ananta, R. Tellgren, and H. Rundlof, J. Eur. Ceram. Soc. **19**, 2667 (1999).
[20] I.-K. Jeong, Phys. Rev. B **79**, 052101 (2009).
[21] S. Tsukada, Y. Hiraki, Y. Akishige, and S. Kojima, Phys. Rev. B **80**, 012102 (2009).
[22] J. Kuwata, K. Uchino, and S. Nomura, Ferroelectrics **37**, 579 (1981).
[23] F. Chu, I. M. Reaney, and N. Setter, J. Appl. Phys. **77**, 1671 (1995).
[24] K. Fujishiro, R. Vlokh, Y. Uesu, Y. Yamada, J. M. Kiat, B. Dkhil, and Y. Yamashita, Jpn. J. Appl. Phys. **37**, 5246 (1998).
[25] G. Xu, P. M. Gehring, and G. Shirane, Phys. Rev. B **72**, 214106 (2005).
[26] M. Iwata, K. Sakakibara, R. Aoyagi, M. Maeda, and Y. Ishibashi, Ferroelectrics **405**, 39 (2010).